A PERFORMANCE-BASED EVALUATION OF INFILL-CONTROLLED LIMIT STATES IN MODERN EUROPEAN RC FRAME STRUCTURES

M. Oliaee[(1)]

[(1)] *Doctoral Student, IUSS Pavia, milad.oliaee@gmail.com*

Abstract

Past earthquakes in Southern Europe have caused damage to external enclosures of unreinforced clay masonry block in RC frame residential buildings. The construction of these buildings in these moderate seismic regions continues, though only with stringent seismic code provisions to mitigate early damage. Analytical tools currently under development by researchers are improving modeling of these buildings, but most studies target the existing building stockpile in their local region. Recent architectural requirements have brought thicker infill walls which are expected to be more resistive to out-of-plane excitation but also effect the in-plane seismic response far more.

Several full scale experiments targeting effects of damage on the out-of-plane response have shown a strong interaction between in-plane drift history and the out-of-plane strength and stiffness. A macro model has been developed and calibrated to the experiment data on different masonry typologies for implementation in nonlinear dynamic analysis. To precisely evaluate the different limit states as prescribed by the Italian National Annex, a full range of the response of the infill is needed--that is, an accurate representation of initial stiffness, the in-plane post-peak behavior, and the collapse of the infill out-of-plane. Local damping of the infill walls out-of-plane direction are updated as damage in the wall progresses.

The damage limitation, ultimate, and collapse prevention limit states are verified by performing time history analyses on an archetype building model subject to a bidirectional ground motion suite with the strong infill typology. The susceptibility of premature damage and expulsion of debris has been estimated using drift indices recorded during the experiment. However, experiments on the wall were not carried out until collapse. Therefore, imminent collapse has been taken as the point at which the infill can no longer resist additional load, which has been shown to change with maximum in-plane drift. Discussion on the significance of the results and the effectiveness of the seismic provisions currently in the design code concludes the study.

Keywords: reinforced concrete frame buildings, nonstructural components, unreinforced masonry infill walls

1. Introduction

1.1 Modern masonry infill construction

Masonry infills in modern RC frame construction constitute a large portion of residential and mixed-used buildings in Italy. In several recent earthquakes, debris has been known to fall from heavily damaged masonry infill panels at serious risk to life safety as shown in Fig. 1 [1, 2]. As architectural requirements for thermal and acoustical insulation have brought an increase to infill wall thicknesses, such components, often considered as non-structural in new design, have come to play a significant role in the global seismic behavior of these buildings. Current seismic design guidelines in the region account for the presence of infills through a modified interstory drift limit based on linear analysis of the RC frame structure; however, the stiffness and strength contribution of infills are usually not included in the analysis, nor are they typically provided to the structural design engineer by the manufacturer.

As part of an effort to advance performance based seismic design and assessment for RC frame buildings with masonry infills, a numerical model intended for dynamic analysis has been proposed, including the out-of-plane response of the infill walls.

Fig. 1 – Observed damage to masonry infills in RC frame buildings following the a) 2009 L'Aquila (left) and b) 2012 Emilia earthquakes

The model uses two experimental campaigns on a thin and thick masonry infill typology to target the effect of in-plane drift demand on the out-of-plane response of infill walls. A relation has been found to occur beyond the in-plane damage limit state at which the stiffness and strength degrade linearly in the masonry. The proposed in-plane/out-of-plane interaction has been compared to the experimental data on the masonry typologies relevant to the region and subject to a suite of bi-directional ground motions scaled to the equivalent seismicity of the damage and life safety performance levels and to observe the effect of the interaction in the dynamic response.

1.1 Previous Infill Models

Since the 1950s infills have been known to interact structurally with the bounding frame [3]. The strut analogy pioneered by Stafford Smith [4] has since been implemented in numerical models with increasing refinement over time. Uniaxial hysteretic rules have been developed for the compression only diagonal trusses specifically for nonlinear dynamic analysis [5].

A model considering the out-of-plane response first appeared in a study comprising the seismic performance of infilled frame buildings, distinguishing between the weak and strong infill typology [6]. Models considering an in-plane and out-of-plane displacement failure surface have evolved over the past decade [7, 8, 9]. A recent implementation (Fig. 2) uses a single strut model with a single fiber hinge at the center of the panel. The model, aimed at analysis for existing buildings, is featured in the structural analysis software OpenSEES [10].

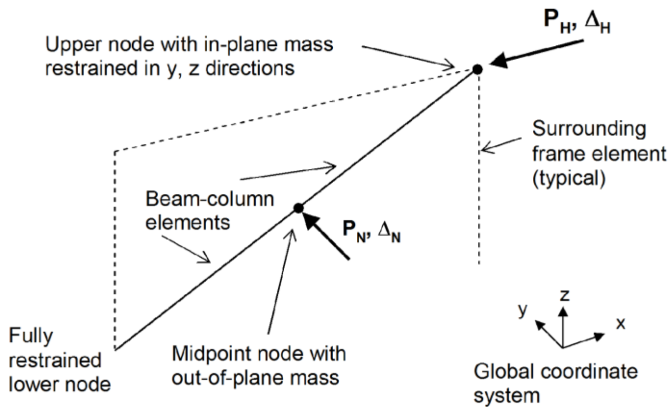

Fig. 2 – Existing infill model with in-plane / out-of-plane interaction currently featured in OpenSEES.

An alternative model to account for damage an asymmetric in-plane response [11, 12] has also been implemented in the open source program. The latter model allows a separation of the out-of-plane stiffness and strength properties from the in-plane element properties; however, the out-of-plane behavior is modelled without any hysteretic behavior or plasticity. Until now, damage to the infill from interstory drift has not been considered to influence the out-of-plane behavior during the analysis. This study incorporates a new model updating the infill wall behavior at the material level for the behavior to match discoveries in more recent experimental campaigns.

2. Experiment Campaigns

2.1 Weak Infill Typology

In 1999, a series of tests were carried out to investigate the effect of reinforcing meshes and bed joint trusses on the seismic strength of infill panels. The study compares the monotonic out-of-plane resistance of unreinforced and lightly reinforced masonry infill walls [13]. Prior to out-of-plane loading, each full scale specimen had been subject to in-plane quasi-static cyclic loading up to 0.4% and 1.2% interstory drift. The masonry infill walls may be classified in the weak infill typology, in that the units have large, horizontal perforations and a smaller unit thickness. The mechanical properties of the individual units and masonry prisms, loaded both vertically and horizontally, are listed in Table 1.

Surveys of damage to the masonry infill wall shown in Figure 3 have been examined to identify the performance limits states of the infill walls. The interaction formula takes advantage of the damage limit state drift index to trigger stiffness degradation in the out-of-plane response.

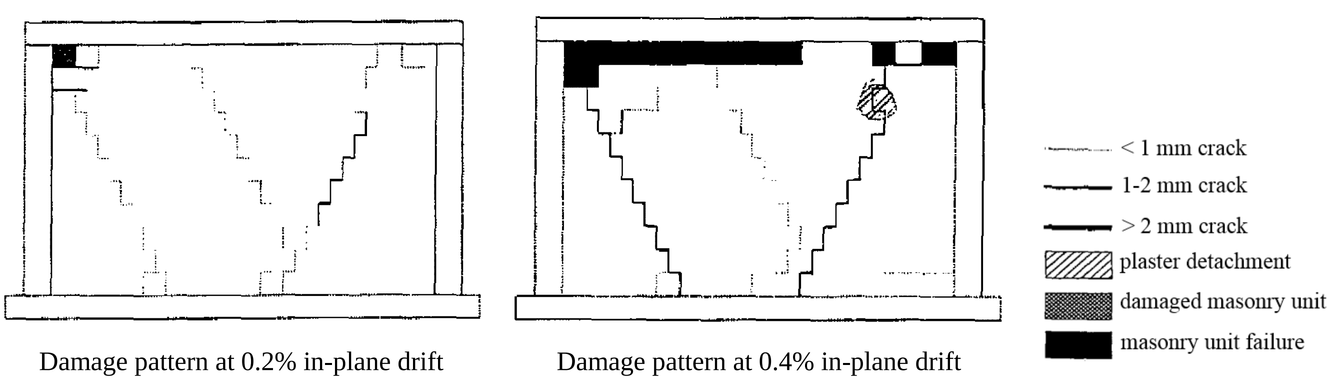

Fig. 3 – The damage patterns for the weak masonry infill typology (Calvi & Bolognini 2001).

The serviceability limit states were reported at load cycles within a 0.4% interstory drift ratio. However, interpretation of the damage and crack patterns per the current seismic provisions would argue the damage limit state occurs at a smaller interstory drift ratio. Eurocode 8 [14] identifies the damage limit state specific to infill walls as the point at which damage to the masonry is reparable and does not require full replacement. According to the damage patterns reported, interpretation of the current code would place the limit state following the cycle at 0.2% drift but before the cycle at 0.4% drift. Therefore, the final damage limitation state has been considered as 0.3% limit with regards to the interaction formula for the weak infill typology.

2.2 Strong Infill Typology

In 2013, an experiment campaign investigated the displacement capacity and shear strength of a new, strong masonry infill typology in the Structural Laboratory at the Department of Civil Engineering and Architecture at the University of Pavia, Italy [15, 16]. The infill panels were loaded out-of-plane, cyclically, at increasing displacement targets in one direction after having undergone different levels of in-plane maximum interstory drift for each specimen.

The strong masonry infill with thick, vertically perforated units has a larger deformation capacity and shear strength with respect to the weak infill typology. The initial stiffness increases an order of magnitude with respect to an RC frame without an infill and ultimate strength is doubled. Prior to the testing of the subassembly, numerous characterization tests were performed on individual units and masonry specimens. The mechanical properties of the masonry from the strong infill typology are listed in Table 1 below. The characteristic values consider 10 masonry units, 6 masonry prisms and 9 triplets.

Table 1 – Characterization of the masonry infills

Typology	Strong Infill		Weak Infill	
Masonry Units	f_b (MPa)	E (MPa)	f_b (MPa)	E (MPa)
Vertical Compression	8.64	9.81	2.80	—
Horizontal Compression	2.78	3.15	15.4	—
Masonry Prisms	f_b (MPa)	E (MPa)	f_b (MPa)	E (MPa)
Vertical Compression	4.64	5299	1.10	1873
Horizontal Compression	1.08	494	1.11	991

For quasi-static cyclic tests on the full-scale subassembly of the RC frame with strong masonry infill, the damage patterns had been recorded following three repetitive cycles at closely spaced in-plane drift targets, shown in Fig. 4. The damage limitation limit state per Eurocode 8 had been identified as 0.5% interstory drift ratio for the fully infill bay. For the infill with opening, the interstory drift ratio corresponding to exceedence of the damage limitation limit state was 0.35%. For the tests on the infill with no opening, the in-plane cyclic tests reached a maximum interstory drift ratio of 2.5%. For the test on the infill with opening, the in-plane cyclic tests reached a maximum interstory dirft ratio of 1.0%. For more information on the experiment data and calibration results from the in-plane cyclic tests, refer to [17].

Following the in-plane tests, unidirectional out-of-plane quasi-static cyclic tests were performed on the infill walls using a 4-hinged apparatus to apply a banded load pattern onto middle third of the wall at midheight. The envelopes of the hystereses from these tests are shown in Figure 8 in the Section 4 during discussion of the model calibration.

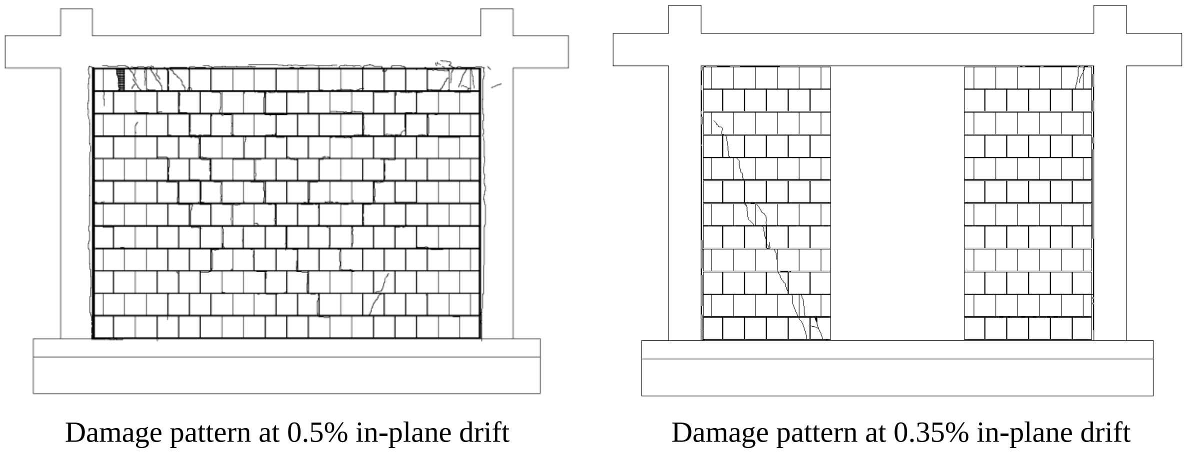

Fig. 4 – The damage patterns at the interpreted damage limit state for the strong masonry infill typology

3. Numerical Model

3.1 Masonry infill model

In an effort to develop a new model and interaction formula to work equally for the strong and weak infill typology, a new model for infills without openings with an assembly of four inclined elements shown in Fig. 5 has two diagonal strut elements (4 and 5) control the in-plane behavior and two modified beam elements (6 and 7) serve for the out-of-plane behavior—without impacting the behavior of the elements providing the in-plane response. The compression-only inelastic truss elements with the original Crisafulli material hysteresis rules and a modified stress-strain constitutive relation. The out-of-plane elements are displacement-based distributed inelasticity fiber elements with axially inextensible constraints. None of the four elements have the capacity to resist tension loads, only compression. Instead kinematic constraints on the extensibility of the fiber elements eliminates their influence on the in-plane response. When subject to double flexure, the fiber elements mimic arching action and resist out-of-plane loads on the central node due to the inextensible element constraints.

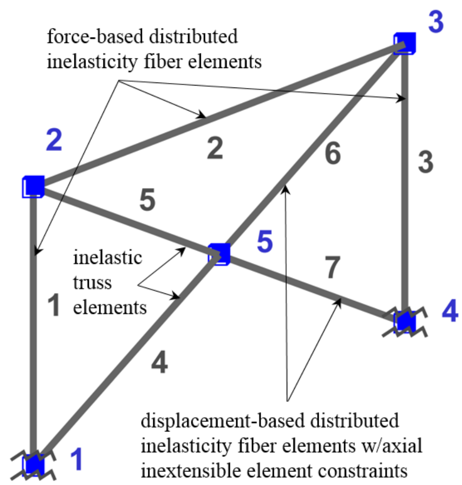

Fig. 5 – The proposed infilled frame model with in-plane/out-of-plane interaction including damage.

The truss elements use a uniaxial material property with a parabolic ascending branch with a constant plateau in compression as shown in Fig. 6. The fiber elements for the weak infill work best using a uniaxial material with a parabolic ascending branch while for the strong infill, a linear ascending branch is used. All the material constitutive relations for the masonry infill assembly have a linear degrading descending branch reaching a residual strength equal to 20% the compressive strength, $0.2f'_m$.

For the in-plane material properties, the ratio of strain at the onset of degradation to the strain at peak strength, $\varepsilon_1/\varepsilon_0$, is greater for the strong infill than for the weak infill, signifying an increase in post-peak displacement capacity. Regardless of typology, the ratio $\varepsilon_0/\varepsilon_u$ remains a constant 2 for the material properties in the fiber elements.

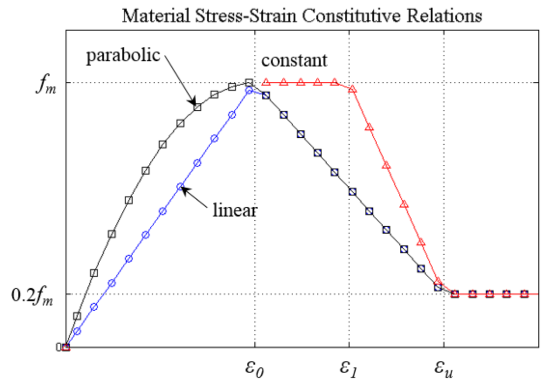

Fig. 6 – Constitutive relations for the masonry infill elements.

3.1.1 In-plane / out-of-plane interaction

The proposed masonry infill element model strictly respects orthogonality of the in-plane and the out-of-plane response. This important aspect allows the interaction algorithm to control the behavior of each element in the assembly. At each increment, the algorithm monitors the maximum in-plane drift and modifies the properties of the fiber elements to reflect the effects of damage on the out-of-plane behavior. In a real earthquake, the seismic response of an infilled frame incurs damage to the masonry through permanent deformation in compression. Likewise, in the model, the material properties in the out-of-plane elements weakens and softens with increasing in-plane drift, by modifying the strain at peak strength of the virgin envelope.

Upon exceeding the damage limit state, the material constitutive relation is modified in the stress-strain domain by amplification of $\varepsilon 0$. Beyond the damage limit state, a reduction in depth of the fiber section accounts for a decrease in the effective wall thickness, in turn weakening the resistance to out-of-plane loads through arching action or bending.

The material constitutive envelope is softened by amplifying the strain at peak strength. The amplification factor is calculated from the ratio of in-plane drift and the drift at the designated damage limit state—concurrent damage observed in the experiments. Eq. (1) gives the simple linear relation:

$$\frac{\varepsilon_{0dmg}}{\varepsilon_{0virg}} = \frac{\delta_{\max}}{\delta_{DL}} \tag{1}$$

where ε_{0dmg} is the strain at peak strength of the damaged material, ε_{0vir} is the strain at peak strength of the virgin material, δ_{max} is the maximum interstory drift and δ_{DL} is damage limit state interstory drift. Initially the fiber elements have a section thickness equal to the infill wall. Beyond the damage limit state, the thickness of the fiber section is reduced to an effective thickness. Equation 2 gives the reduction in section depth or thickness, t_{red}, initiating at a drift limit equal to twice the damage limit interstory drift ratio.

$$t_{red} = 0.1\left(\frac{\delta_{\max}}{\delta_{DL}} - 2\right) \geq 0 \qquad (2)$$

For each of the three strong infill specimens, significant damage occurred in the infill wall at a drift ratio around 1.0%. Images of units losing outer shells after having undergone in-plane deformation are shown in Fig. 7. The material loss from the outer shells of the masonry units would indicate a reduction in effective thickness capable of reducing out-of-plane resistance via arching action.

a) Specimen TA1 b) Specimen TA3

Fig. 7 – Observed damage to masonry infills after 3 repeated reverse cycles at 1.0% in-plane drift

4. Calibration

4.1 RC Frame Elements

The reinforced concrete elements developed in the program are force-based distributed inelasticity fiber elements [18] with four Gaussian integration points [19]. The concrete uniaxial fibers follow Mander's rule [20] on the ascending branch with a modified Kent-Park unloading hysteresis [21]. The longitudinal steel reinforcement use the popular Giuffré-Menegotto-Pinto material model [22] with the Bauschinger effect. The RC frame reinforcement scheduling and detailing of the specimens follow the seismic code provisions for ductile behavior at the time of construction.

4.2 Masonry Infill Material Input Properties

The material input properties for the infilled frame finite element model are listed in Table 2. The area of the diagonal trusses are 0.45 m^2 and 0.21 m^2 for the strong and weak infill models, respectively.

Table 2 – Input properties for infill elements.

Floor Level	Strong Infill				Weak Infill			
Ground (5 m bay)	f_m (kPa)	E (MPa)	ε_0 (10^{-3})	d_w (m)	f_m (kPa)	E (MPa)	ε_0 (10^{-3})	d_w (m)
Truss Elements	618	122	4.7	1.4	99	56	0.4	0.8
Fiber Elements	4764	5299	1.0	3.6	1254	3550	0.4	3.6

Further information on the material properties and hysteretic properties for the in-plane response of RC frames with the strong infill typology may be found in [7].

4.3 Loading Procedure

P-delta effects in the vertical RC columns and diagonal fiber elements are considered. A displacement-based multi-step incremental analysis compares the specimen response to quasi-static loading. A vertical load of 400 kN on each column is held constant for both the in-plane and out-of-plane loading, shown in Fig. 8.

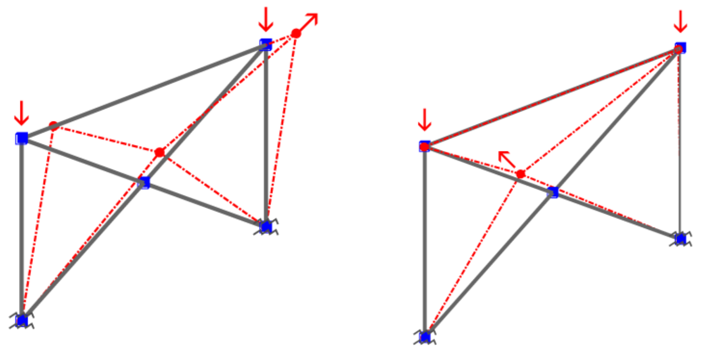

Fig. 8 – Sequential loading of numerical model: in-plane displacement-controlled reverse cyclic loading followed by unidirectional out-of-plane cyclic loading

For both the weak and strong typology, numerical models of the experiment specimens have been created to calibrate the interaction formula. The results show an increase in maximum out-of-plane displacement at peak resistance (Fig. 9) numerically achieved by softening the stress-strain constitutive relation in the fiber elements. The decrease in out-of-plane strength capacity has been captured by reducing the effective thickness of the wall.

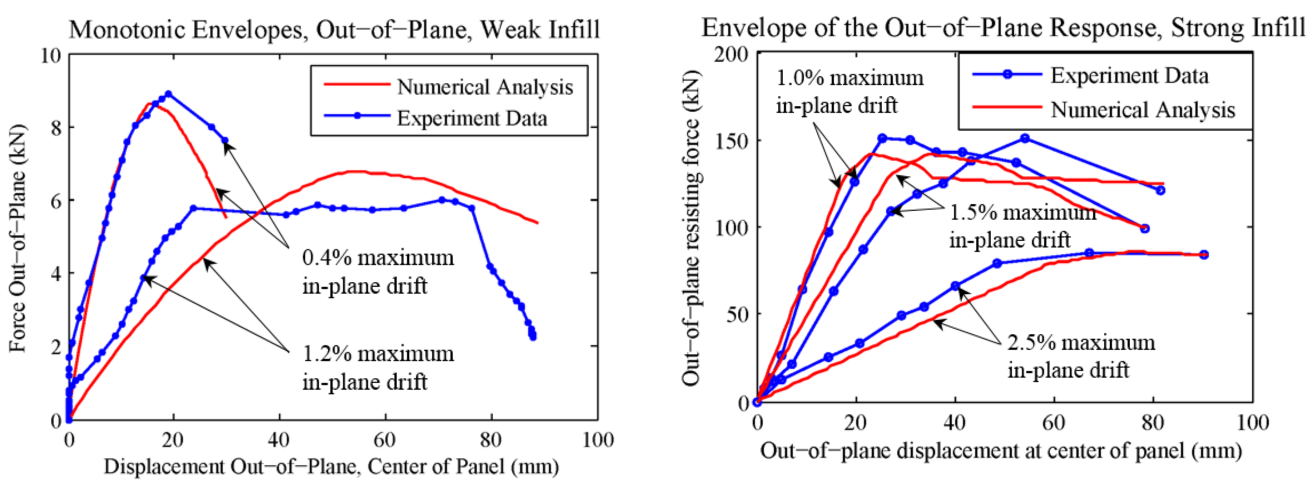

Fig. 9 – Comparison of the experiment data and numerical model of the infilled frame specimen with the weak (left) and strong (right) infill typology loaded in the out-of-plane direction

5. Performance Assessment

5.1 Archetype Model

In order to accurately assess the performance of the modern RC frame construction with strong masonry infill walls, a 6 story building has been subject to a suite of bi-directional ground motions at varying seismic intensity. The buildings have been designed according Eurocode 8 with the Italian National Annex [23] carefully considering the drift limit requirements for building with infills, shown in Fig. 10 below. The building has a high ductility class and moment frames in both directions along each frame line. The planar frame model represents an interior frame line of a modern RC frame building. Column widths of the first 3 stories are 45 cm thick and 35 cm thick for the last 3 stories with 3 #22 metric bars on each face.

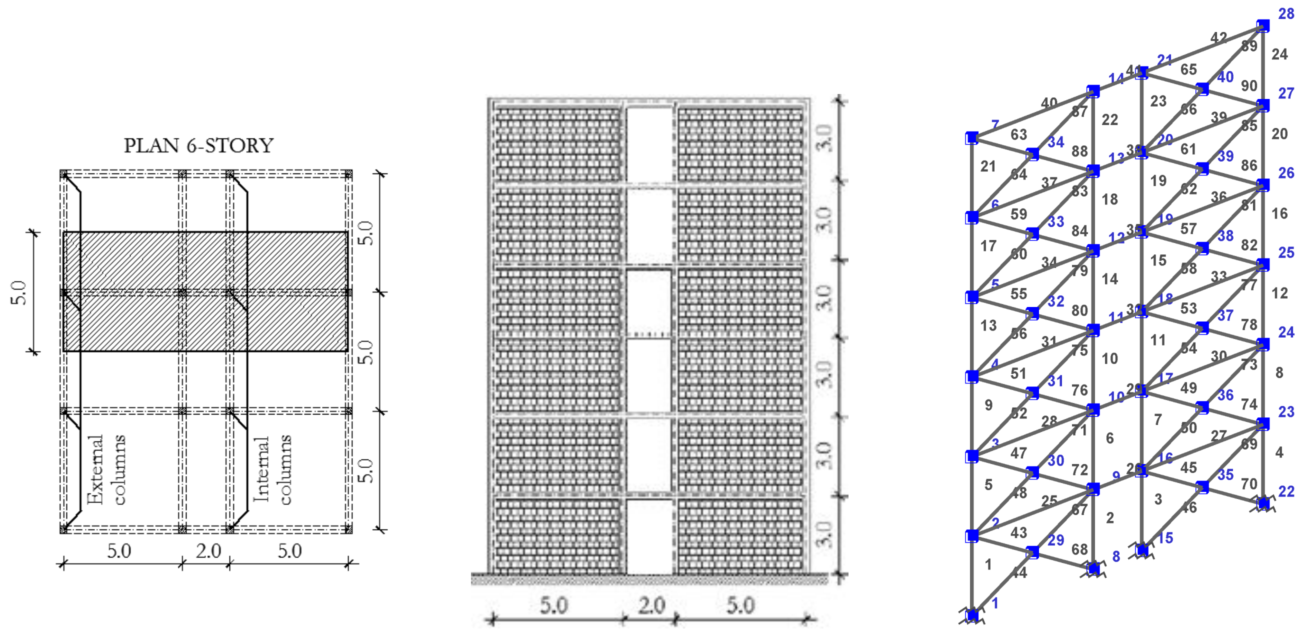

Fig. 10 – Plan, elevation, and isometric of 6-story building model with masonry infill elements shown

Although the building model is a 2D planar structure, it's model space has three dimensions. The infill masses can move freely out-of-plane and are subject to amplified ground motions based on the mid-height of the story. The analysis is iterative, in that the peak floor acceleration (PFA) amplification with respect to the ground motion peak ground acceleration (PGA) are taken from previous run until the values converge. On average there is a peak acceleration amplification factor of 3.5 at the roof. This analysis methodology was chosen out of convenience because the numerical model and nonlinear dynamic analysis solver were developed in Matlab [24] for testing purposes and require more computational time than typically accepted for time history analysis of 3D spatial models.

5.2 Ground Motion Selection and Scaling

Thirteen ground motions have been selected—10 from the far field ground motions in Appendix A of FEMA p695 [25] and 3 of the highest magnitude earthquakes in Italy from the ITACA database [26]. Before scaling, the ground motions are normalized by the median PGV. The damage limitation, ultimate, and collapse prevention limit states each have a 50, 475, and 975 year return period, respectively. The Eurocode 8 design response spectrum is anchored to PGA, so each record has been shown in Table 3 listing the scale factors for attaining the PGA representing the three levels of seismicity after normalization. The maximum PGA considered for the life safety limit state is 0.47 g PGA (0.35gS) for soil class D.

Table 3 – Bidirectional ground motion suite with scale factors.

Ground Motion (RSN)	0.19 g PGA	0.47 g PGA	0.56 g PGA
Northridge (953)	0.36	0.90	1.08
Duzce (1602)	1.13	2.79	3.35
Hector (1787)	0.81	2.00	2.40
Kobe (1111)	3.08	7.60	9.12
Kocaeli (1158)	1.88	4.63	5.56
Loma Prieta (752)	0.38	0.92	1.10
Manjil (1633)	0.55	1.35	1.62
Super Hills (718)	0.53	1.30	1.56
Chi Chi (1485)	0.42	1.03	1.24
San Fernando (68)	0.65	1.59	1.91
Friuli (125)	0.49	1.20	1.44
L'Aquila (4547)	0.51	1.27	1.52
Irpinia (288)	0.49	1.22	1.46

5.3 Performance Criteria

Each performance level may be satisfied if the median response stays within prescribed limits. For the damage limitation limit state, the maximum interstory drift shall not exceed 0.5%. For the ultimate limit state, all infill walls shall avoid imminent collapse out-of-plane. Although the experiment tests did not continue until failure, the walls reached their peak resistance and began to degrade rapidly. During the tests, imminent collapse of an infill could occur at different out-of-plane displacements depending on the maximum in-plane drift imparted to the infill beforehand. Therefore, the collapse criteria and element removal algorithm are updated by the maximum recorded interstory drift during the analysis for each infill. For the collapse prevention limit state, infills may collapse so long as the RC frame structure can continue to support gravity loads.

5.4 Results

The maximum interstory drift ratios for each infill was recorded. The median drift ratio was compared to each performance level at each corresponding seismic intensity. The particular configuration of infill wall placement and infill typology of the model has provided interesting results. The median and maximum recorded interstory drift ratios are provided below in Table 4 for each performance level. The in-plane drift ratios are with respect to the centerline frame height whereas the out-of-plane drift ratios are with respect to the clear height of the frame.

The strong infill does well to limit global in-plane drift ratios by adding stiffness and strength to each story level; however, response is amplified for the infills in the orthogonal direction. Excitation of the wall masses out-of-plane cause can cause significant deformations, although within limits for the median response. The time history with the Kocaeli earthquake scaled to the life safety limit state had infills collapsing at the 5th floor, subsequently changing the drift profile up the building and concentrating deformation at that story. Although the PFA amplification at the top floor is more significant, damage incurred from in-plane drifts at lower stories caused by softening out-of-plane. The effect was enough for those infill walls to exceed their collapse limits sooner.

Table 4 – Maximum Interstory Drift Ratios

	In-Plane	Out-of-Plane
Performance Level	median (%)	median (%)
Damage Limit	0.13	0.17
Life Safety	0.42	0.46
Collapse Prevention	0.57	0.56

5. Conclusions

In an effort to evaluate the effectiveness of existing seismic provisions for masonry infilled RC frame buildings in seismically prone regions in Europe, an archetype building model with a new macro-model has been developed and calibrated to experiment data relevant to the region. Damage and collapse of the infills has been monitored in the building for a batch of time history analyses considering the nonlinear behavior of the unreinforced masonry infill walls. The building was subject to bidirectional strong ground motions normalized to the PGV and scaled to the maximum PGA considered for design in Italy. Three levels of seismicity for limit state verifications found in the Italian National Annex have been considered. The strong infill walls had no openings and did not incur significant damage at the 50 year return period (or damage limit) intensity, nor did infills collapse at the 475 year return period (or life safety) limit state.

As the existing building stockpile of infilled frame buildings continues to grow across the world, a more powerful numerical tool to help estimate drift demand and model building response will help structural engineers counter the seismic risks they present to the public. The model introduced in this study has shown promising results in comparison to experiment data on a weak and strong infill typology in Italy. More experiment data targeting the change in the out-of-plane response from in-plane damage is needed to verify the proposed model.

4. Acknowledgements

Partial funding from the Reluis-DPC framework program 2015 RS 12-Masonry Infills is gratefully acknowledged.

5. References

[1] Ricci, P., De Luca, F., Verderame, G. M. 2011. 6th April 2009 L'Aquila earthquake, Italy—reinforced concrete building performance. Bulletin of Earthquake Engineering 9(1): 285-305.

[2] Penna, A., Morandi P., Rota, M., Manzini, C., Porto, F., Magenes, G. 2012. Performance of masonry buildings during the Emilia 2012 earthquakes. Bulletin of Earthquake Engineering 12:2255-2273.

[3] Polyakov, S.V. 1956. Masonry in framed buildings. Watford, UK: Building Research Station.

[4] Stafford Smith, B. 1966. Behavior of square infilled frames. American Society of Civil Engineers proceedings 381-403.

[5] Crisafulli. F., Carr, A. & Park, K. 2000. Analytical modelling of infilled frame-structures—a general review. Bulletin of Earthquake Engineering 137:1508-1517.

[6] Fardis, M.N. 1996. Experimental and numerical investigations on the seismic response of R.C. infilled frames and recommendations for code provisions. Lisbon, Portugal: Laboratorio Nacional de Engenharia Civil.

[7] Hashemi, A & Mosalam, K.M. 2007. Seismic evaluation of reinforced concrete buildings including effects of masonry infill walls. Berkeley, USA: Pacific Earthquake Engineering Research Center.

[8] Kadysiewski, S. & Mosalam, K.M 2008. Modeling of unrein-forced masonry infill walls considering in-Plane and out-of-plane interaction. Berkeley, USA: Pacific Earthquake Engineering Research Center.

[9] Mosalam, K.M. & Gunay, S. 2015. Progressive collapse analysis of RC frames with URM infill walls considering in-plane/out-of-plane interaction. Earthquake Spectra.

[10] McKenna, F. 2011. OpenSEES: a framework for earthquake engineering simulation. Computing in Science & Engineering 13(4):58-66.

[11] Rodrigues, H., Varum, H., & Costa, A. 2010. Simplified macro-model for infill masonry panels. Journal of Earthquake Engineering 14:390-416.

[12] Furtado, A., Rodrigues, H., & Arede, A. 2015. Simplified macro-model for infill masonry walls considering the out-of-plane behaviour. Earthquake Engineering & Structural Dynamics.

[13] Calvi, G.M & Bolognini, D. 2001. Seismic response of rein-forced concrete frames infilled with weakly reinforced ma-sonry panels. Journal of Earthquake Engineering 5:153-185.

[14] CEN Eurocode 8 2013. Design of structures for earthquake resistance, Part 1: General rules, seismic action and rules for buildings. Brussels, Belgium: European Committee for Standardisation.

[15] Morandi, P., Hak. S., & Magenes, G. 2014. In-plane experi-mental response of strong masonry infills. International Masonry Conference.

[16] Hak. S., Morandi, P., & Magenes, G. 2014. Out-of-plane exper-imental response of strong masonry infills. European Conference on Earthquake Engineering and Seismology.

[17] Oliaee, M., Morandi, P., & Magenes, G. 2015. Macro model calibration of a strong clay masonry infill to in-plane cyclic tests. International Conference on Computational Methods in Structural Dynamics and Earthquake Engineering.

[18] Taucer, F.F, Spacone, E., & Filippou, F.C. 1991. A fiber beam-column element for seismic response analysis for rein-forced concrete structures. Berkeley, USA: Earthquake Engineering Research Center.

[19] Thompson, H.B., & Tuttle, C. 1984. Basic Tools: Integration by Gaussian Quadrature. Journal of Computers in Mathematics and Science Teaching 3(3) 43-44.

[20] Mander, J.B., Priestley, N.M, & Park, R. 1988. Theoretical stress-strain model for confined concrete. Journal of Structural Engineering 113(8): 1804-1825.

[21] Scott, B.D., Park, R., & Priestley, M.J.N. 1982. Stress-strain behavior of concrete confined by overlapping hoops at low and high strain rates. Journal of the American Concrete Institute 79(1): 13-27.

[22] Menegotto, M., & Pinto, E. 1973. Method of analysis for cyclically loaded reinforced concrete plane frames including changes in geometry and non-elastic behavior of elements under combined normal force and bending. International Association for Bridge & Structural Engineering Proceedings.

[23] NTC 2008. Norme techniche per le costruzioni. Rome, Italy: Ministero dell Infastrutture.

[24] MATLAB version 8.2.0. Natick, Massachusetts: The MathWorks Inc., 2013.

[25] FEMA p695. 2009. Quantification of Building Seismic Performance Factors. Applied Technology Council, Redwood City, California.

[26] Luzi, L., S. Hailemikael, D. Bindi D, F. Pacor, F. Mele, F. Sabetta (2008), *ITACA (ITalian ACcelerometric Archive): A Web Portal for the Dissemination of Italian Strong-motion Data*, Seismological Research Letters, 79(5), 716–722.